

614 A 3D RANS APPROACH BASED ON A MODIFICATION OF THE EFFECTIVE PRANDTL NUMBER FOR HIGH RESOLUTION MESOSCALE SIMULATIONS

Alberto Martilli*
CIEMAT, Spain

Rich Rotunno¹, Jason Ching², Peggy Lemone¹

¹ NCAR, Boulder CO; ² Institute for the Environment, The University of North Carolina, Chapel Hill, NC, USA

1. INTRODUCTION

Thanks to the continued increase of computational power, it is now common to perform mesoscale simulations with spatial resolution of less than one kilometer to better resolve circulations induced by surface spatial heterogeneities of few kilometers (like cities, lakes, or narrow valleys). However, standard PBL closures in convective conditions generate spurious circulations that have shapes similar to convective rolls or cells, but do not always have the same size, do not necessarily form in the same conditions and are grid resolution dependent (we will call them Modeled Convectively Induced Secondary Circulations, M-CISC). Given this, it is likely that the resulting M-CISCs are model artifacts.

To understand this problem, the classical theory of Rayleigh (1916) can be used to investigate the onset of the M-CISCs (Ching et al. 2014, and paper 13.3 of this meeting). By replacing the viscosity and thermal diffusivity by the correspondent *eddy* viscosity, n , and *eddy* thermal diffusivity, k_H produced by the PBL schemes, it is possible to form an effective Rayleigh number (Ra_{eff}) as

$$Ra_{eff} = \frac{b^2 H^4}{nk_H} \quad (1)$$

where $b^2 = -\frac{g}{q_0} \frac{\partial q}{\partial z}$ H is the depth of the super-adiabatic layer. M-CISCs form when $Ra_{eff} > Ra_{cr}$. From the modelling point of view, the problem is that Ra_{cr} is grid size dependent. In fact, if we assume that k_H and n are the same in the horizontal and vertical

directions it can be shown (Ching et al. 2014) that

$$Ra_{cr} = \frac{P^4}{\left(\frac{I_x}{2H}\right)^4} \left(1 + \left(\frac{I_x}{2H}\right)^2\right)^3 \quad (2)$$

where I_x is the horizontal scale of the convective structure¹.

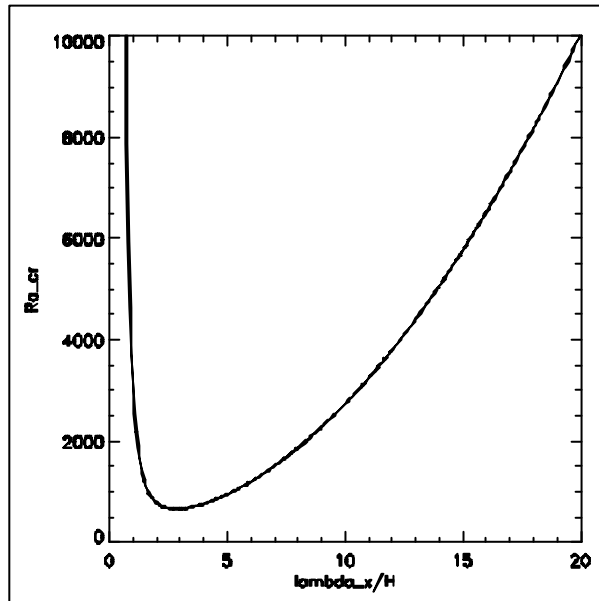


Figure 1. Ra_{cr} as a function of I_x .

However, in a numerical model, I_x has a lower limit imposed by the numerical resolution. Since the smallest motions that a simulation with grid spacing Δx can resolve are $4-8 \Delta x$ (depending on the quality of the advection scheme) the minimum $I_{xMIN} \approx \alpha \Delta x$ with α between 4 and 8. As a

*Corresponding author: Alberto Martilli, CIEMAT, Department of Environment, Avenida Complutense, 40, 28040 Madrid, Spain; e-mail: alberto.martilli@ciemat.es

¹ Expression (2) is valid only if the horizontal and vertical eddy diffusivities are equal, but qualitatively similar analysis can be done when this is not the case.

consequence, Ra_{cr} for a simulation with grid spacing Δx is the minimum of (2) for $I_x > I_{xMIN}$. Graphically it is the minimum of the curve represented in Fig. 1, to the right of the value of $\frac{I_{xMIN}}{H}$ corresponding to the resolution of the simulation. For example, in typical convective conditions (see for example Shin and Hong, 2011) $H=500m$, $\frac{\partial q}{\partial z} = -0.001K/m$, and averaged values of eddy diffusivities of the order of $n \approx k_H \approx 30m^2s^{-1}$, which implies $Ra_{eff} = \frac{b^2 H^4}{nk_H} = 2200$. From an inspection of Fig. 1, it can be easily seen that when $\frac{I_{xMIN}}{H} \approx 15$ (e. g. grid size of more than one km), $Ra_{eff} < Ra_{cr}$, but when $\frac{I_{xMIN}}{H} \approx 5$ (e. g. grid size of several hundreds of meters), $Ra_{eff} > Ra_{cr}$.

To better understand how to tackle this problem it is important to clarify the averaging operator used to filter the equations of motions. The two most common approaches are:

Volume averaging.

Volume average over the numerical grid cell:

$$\bar{u} = \frac{1}{\Delta x \Delta y \Delta z} \int_{x-\Delta x/2}^{x+\Delta x/2} \int_{y-\Delta y/2}^{y+\Delta y/2} \int_{z-\Delta z/2}^{z+\Delta z/2} u(x, y, z, t) dz dy dx$$

This is the averaging adopted in classical mesoscale textbooks like Pielke, (1984), and it is similar to the averaging used in Large Eddy Simulations. It filters out all structures smaller than the grid cell. The effect of the subgrid motions must be parameterized with formulations that must be a function of the grid size (as it is in LES).

Ensemble averaging

The ensemble average or mean (the operator used in classical turbulence theory) can be defined as (Pope, 2000)

$$\bar{u}(\vec{x}, t) = \int_{-\infty}^{\infty} v f(v) dv$$

Where $f(v)$ is the probability density function. So, the mean is the probability-

weighted average of all possible values that a variable $v(x,t)$ can take. The aim of this average is to filter all the turbulent components (which are random and therefore unpredictable), and leave only the non turbulent part of the fields (which are therefore predictable). In this type of models, turbulence is completely parameterized and only the mean field is resolved. The filter is on the nature of the atmospheric structures (random vs non-random), and not on their size. Models using this approach are called RANS (Reynolds Averaged Navier Stokes) models.

The PBL schemes used in current mesoscale models are a mix of the two approaches: in the vertical they are based on ensemble averages (Mellor and Yamada, 1974), while in the horizontal the diffusion coefficients are based on the flow deformation and the grid size (Smagorinsky schemes, same type of schemes used in LES).

For resolution of several kilometers, this confusion in the definition it is not considered a problem because within one grid cell there can be several turbulent structures, so the ensemble average can be approximated by the volume average. However, at sub-kilometer resolutions, a choice must be made between the two averaging operators. If the volume average is chosen, as explained in Wyngaard (2004), the problem is that, since the size of the filter is comparable with the turbulent length scales, the traditional LES closures cannot be used, and there are currently no approaches adapted (it is a "Terra Incognita"). In this investigation, we examine the results when applying the other approach, e.g. consider the ensemble averaging operator.

2. PROPOSED SCHEME

As the daytime-heating cycle begins, the ground temperature rises faster than that of the overlying atmosphere, creating an intense near-surface superadiabatic layer. In these conditions, a small perturbation can start convective motions that can take the form of rolls or cells, depending on the ratio z_i/L (where z_i is the height of the PBL; and L is the Monin-Obukhov Length). These **real** features (that we will call Convectively Induced Secondary Circulations, CISC), are random in nature, and an ensemble-average operator should filter them out.

The aim of the proposed scheme is to parameterize the effect of CISCs, and avoid the formation of M-CISCs.

As explained in the introduction, M-CISCs form when $Ra_{eff} > Ra_{cr}$. From the physical point of view, Ra_{eff} can be seen as the ratio between the timescale of the diffusion processes

$$t_{diff} = \frac{H^2}{k_H}$$

over the time scale of the buoyancy induced (e. g. convection) processes

$$t_{buoy} = \frac{n}{b^2 H^2}$$

When the time scale of the buoyancy becomes significantly smaller than the time scale of the diffusion ($Ra_{eff} > Ra_{cr}$), the model finds generates vertical motions (e. g. the M-CISC) to transfer the heat vertically rather than diffusing it.

From (2) the value of Ra_{cr} can be computed as the minimum that the expression

$$Ra_{cr} = \frac{p^4}{\left(\frac{n\Delta x}{2H}\right)^4} \left(1 + \left(\frac{n\Delta x}{2H}\right)^2\right)^3$$

takes for $n=1, N$, with N number of grid points.

The idea is to use the same coefficients in the horizontal and the vertical directions (e. g. $n_x = n_z$) and to modify the effective Prandtl Number

$$Pr_{eff} = \frac{n}{k_H}$$

to keep Ra_{eff} below the critical value. This gives

$$Pr_{eff} = \min\left(1, Ra_{cr} \frac{\bar{n}^2}{b^2 H^4}\right)$$

Since the eddy diffusivity is not constant with height, an average value over H has been used following $\frac{1}{\bar{n}} = \frac{1}{H} \sum_{i=1, NH} \frac{\Delta z_i}{n_i}$,

where n_i is the diffusivity at level i , Δz_i is the depth of level i , and NH is the number of grid points within the superadiabatic layer. This is equivalent to ensure that the diffusion mechanism is always more efficient than the generation of vertical motions to transfer heat upward. We will call this new scheme PR3D. The modification to the Prandtl number is computed for every column and applied from the surface to the top of the domain.

The efficiency of this technique is tested in WRF by modifying the Bougeault and Lacarrere (1989, BouLac hereafter) PBL closure scheme. BouLac computes the eddy

viscosity and thermal diffusivity in the vertical direction as:

$$n_z = C_k l_k \sqrt{tke}$$

$$k_{Hz} = n_z$$

where C_k is a constant equal to 0.4, and l_k is a length scale estimated as a function of the local value of turbulent kinetic energy (computed by solving a prognostic equation) and the entire vertical profile of potential temperature.

3. TESTS OVER HOMOGENEOUS SURFACES.

As first test for the scheme, two simulations with flat terrain and spatially homogeneous surface heat flux, constant with time, are considered. The expected results are horizontally homogenous meteorological fields, since the CISCs, for their random nature, should not be visible in the output of an ensemble averaged model. Results are compared against simulations with the STANDARD approach, always with BouLac, but with $Pr_{eff}=1$ (as in the original formulation), eddy viscosity and thermal diffusivity in the horizontal estimated following the Smagorinsky approach based on the deformation of the flow, as recommended in WRF,

$$n_x = C_s^2 \Delta x^2 \left[0.25 \left(2 \frac{\partial U}{\partial x} - 2 \frac{\partial V}{\partial x} \right)^2 + \left(\frac{\partial U}{\partial x} + \frac{\partial V}{\partial x} \right)^2 \right]$$

$$k_{Hx} = 3n_x$$

with $C_s=0.25$.

Three spatial resolutions are considered:

1km, 500m and 250m.

Cells

The first set of simulations is characterized by $Z_i/L=-100$ (L is Obukhov length), a typical regime where convective cells form. Surface heat flux is 285 W/m^2 , geostrophic wind speed is 5m/s from the west (left in the figures), and roughness length is $z_0=0.1 \text{ m}$. The initial conditions are characterized by a neutral profile until 1000m , and a strong capped inversion. Horizontal fields of vertical velocity at 400m above the ground after 5 h of simulations are presented in Fig. 2, for the STANDARD approach and for PR3D. It is clear from the graphs that STANDARD produces M-CISCs of a size that

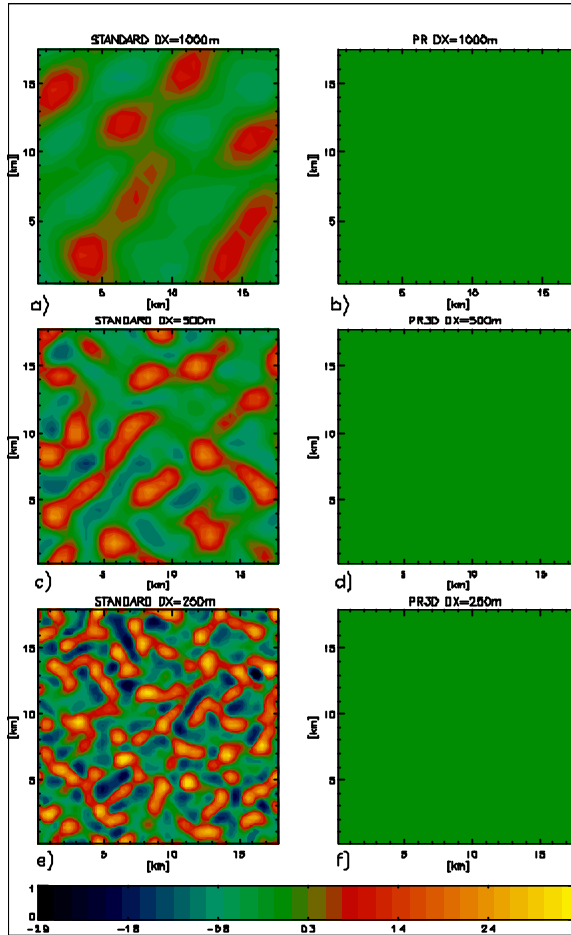


Figure 2. Vertical velocity at 400m a.g.l. for $z_i/L=100$.

decreases with grid size. Moreover, the vertical velocity increases with resolution. On the other hand, PR3D does not show any structure.

Rolls

The second set of simulations is for $Z_i/L=10$, typical for the formation of convective rolls. The surface heat flux is 100 W/m^2 , the geostrophic wind speed is 20 m/s , $z_0=0.1 \text{ m}$. Results after 5 h of simulation are shown in Figure 3, again for vertical velocity at 400m above ground. From the figures it is clear that STANDARD produces rolls both at 500m and 250m resolution, but with different orientation, wavelength and intensity of vertical velocities. On the other hand PR3D produces homogeneous fields.

In summary, in both cases, STANDARD generates M-CISCs of shape and intensity that changes with the resolution, while PR3D always produce horizontally homogeneous fields, as it should be expected from a RANS scheme.

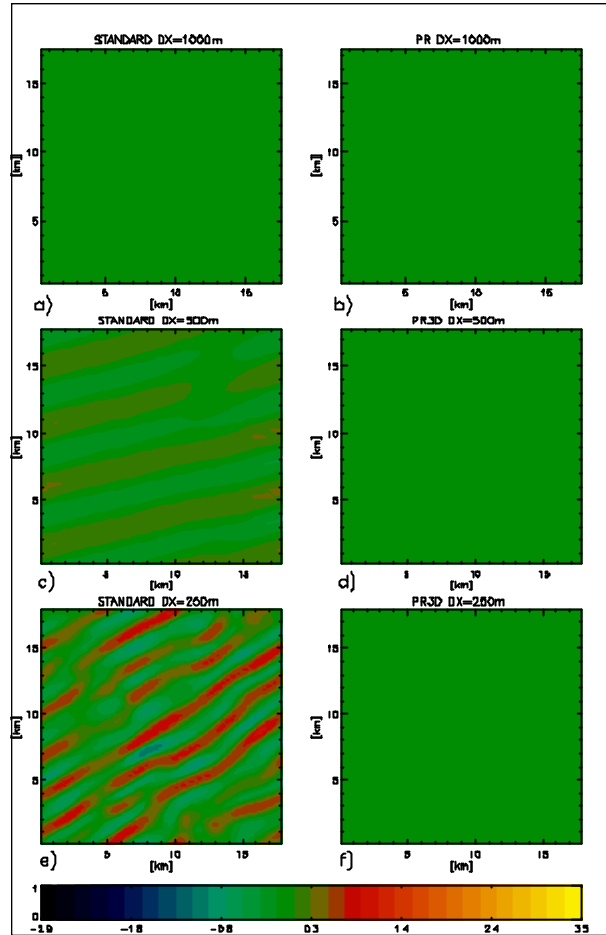


Figure 3 Vertical velocity at 400m a.g.l. for $z_i/L=10$.

To assess more quantitatively the new scheme, vertical profiles of potential temperature are compared against horizontal spatial averages from LES simulations obtained with WRF-LES with a resolution of 30m (for more details, see Ching et al. 2014). Here the horizontal spatial averages from LES are considered equivalent to ensemble mean. The shape of the profiles produced by PR3D is very similar to those obtained with LES under identical conditions.

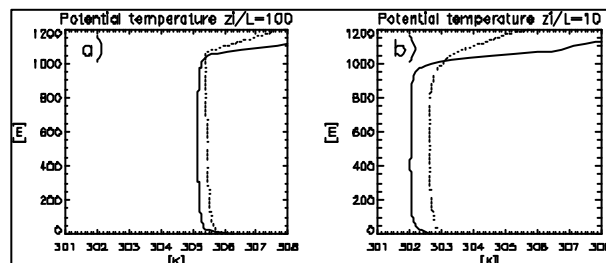


Figure 4 Vertical profiles of potential temperature from PR3D (dotted), and the horizontal spatial average of LES (solid)

4. TESTS OVER HETEROGENOUS SURFACES.

One of the main purposes of PR3D is that it should be able to resolve ensemble mean circulations induced by surface flux heterogeneities. To assess this, two further cases are simulated:

2D Lakes.

On a flat domain 16kmX16km, two kilometers wide stripes of surface with heat flux of 0.24 K m s^{-1} (representing land) are alternated with 2 km wide stripes with zero surface heat flux (representing lakes) as indicated in Figure 5

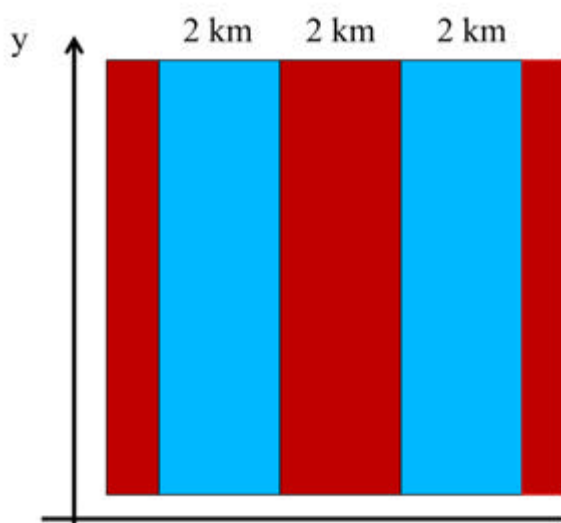


Figure 5 Domain of the 2D Lakes and 2D city runs. Land is indicated in red, and water in blue for the “lake” runs. Similarly, rough and hot surfaces are in red, and smooth and cool surfaces are in blue for the “city” runs.

Spatial resolution in the horizontal is 200m and in the vertical is 15m constant with height. Initial conditions for potential temperature profiles are the same as for the homogenous test cases, except initial wind speed is 1 m s^{-1} . Periodic boundary conditions are used in the horizontal. Given the homogeneity in the Y (north-south) direction, the ensemble mean is expected to be also homogeneous in that direction. This is what is obtained with PR3D (Fig.6). On the other hand, STANDARD, applied to the same case, does not produce homogeneous fields in Y.

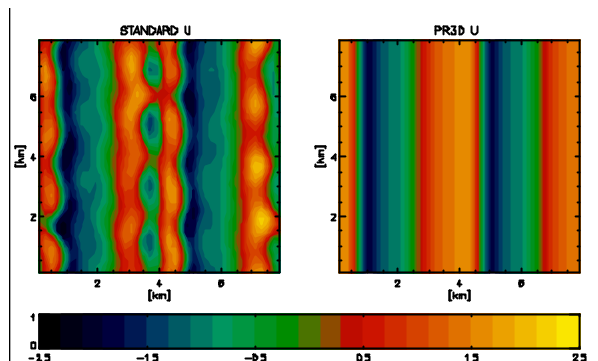


Figure 6 Horizontal section of U at 7m a.g.l. for the 2D Lakes case for STANDARD (left) and PR3D (right).

To better evaluate the behavior of the scheme, WRF in LES mode has been run over the same domain, with a spatial resolution of 40m in the horizontal and 15m in the vertical, and the same initial and boundary conditions. Due to the homogeneity in the Y direction, spatial averages over Y are considered representatives of the ensemble mean, and can be compared to the results of PR3D. Furthermore the LES results averaged over Y have been averaged also every 200m, to get fields comparable to those produced by PR3D at 200m resolution. A vertical section of potential temperature and horizontal component of the wind is represented in Fig. 7, and compared with those computed by PR3D. Wind speed and potential temperature at the lowest model level (7 m a.g.l.) are also plotted in Fig. 8.

While PR3D is able to reproduce the lake breezes in the right position and with the right intensity close to the surface, the vertical extension of the breeze, and intensity of the return current is underestimated.

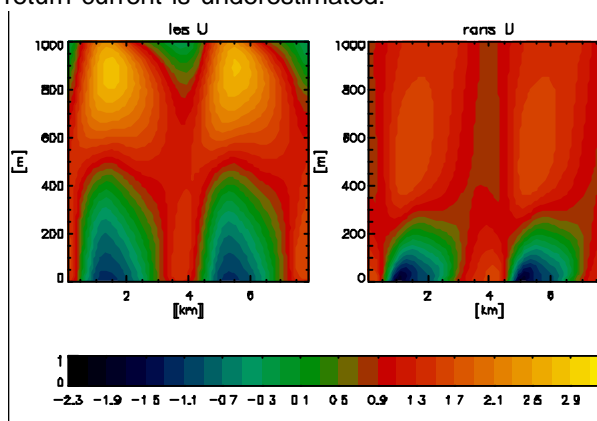


Figure 7a. Vertical section for the lake case for U for LES (left) and PR3D (right).

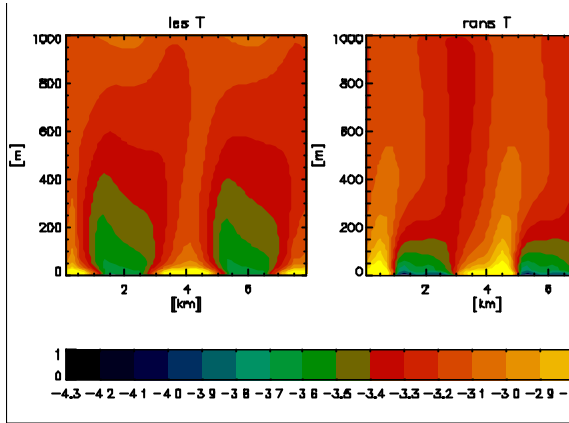


Figure 7b. Vertical section for the lake case for perturbation of potential temperature for LES (left) and PR3D (right).

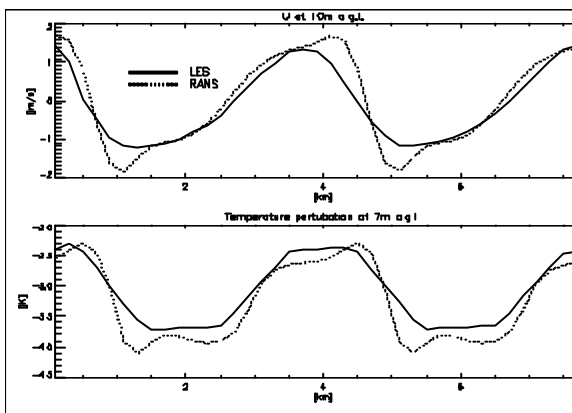


Figure 8 U and perturbation of potential temperature at the lowest model level (7m above ground) for the Lake case along X.

2D cities

A second test similar to 2D lakes has been realized, but with a 2 km wide strip of land rougher and with heat flux of 0.36 K m/s, representing a city, alternated with a strip smoother and with lower heat flux (0.12 K m/s) representing a rural area. All the other conditions are similar to the 2D Lakes case. What is aimed with this test is to challenge the scheme with a situation with stronger convection. Conclusions from these results are similar to those obtained for the 2D Lakes cases (see Fig. 9,10 and 11). STANDARD produces fields that are even more heterogeneous in the Y direction than in the previous case, while PR3D is homogenous in Y. The comparisons against spatially averaged LES results indicate that PR3D is able to reproduce relatively well the wind speed close to the ground (but with a shift of few hundreds of meters) and the potential temperature. But it underestimates the depth of the circulation and the intensity of the return current, as in the previous case. In

addition, the vertical profiles of potential temperature are quite different than LES, in particular above the rough and hot surfaces (Figure 10b).

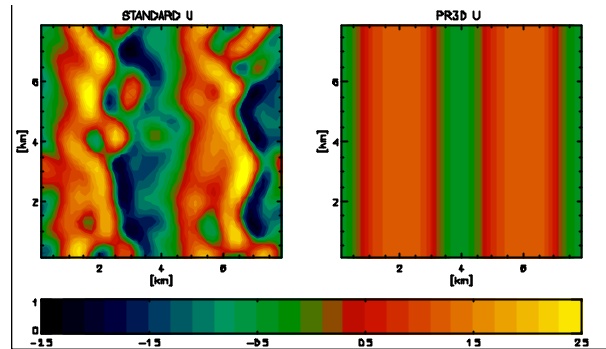


Figure 9 Horizontal section of U at 7m a.g.l. for the city case

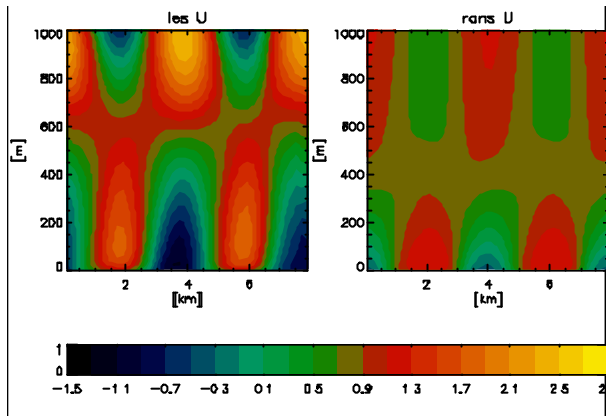


Figure 10a. Vertical section for the city case for U for LES (left) and PR3D (right).

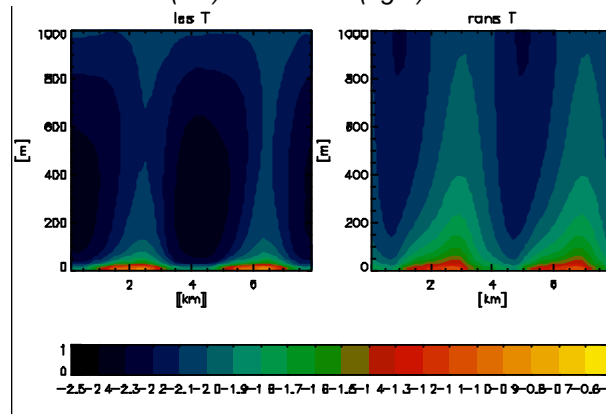


Fig 10b. Vertical section for the city case for perturbation of potential temperature for LES (left) and PR3D (right).

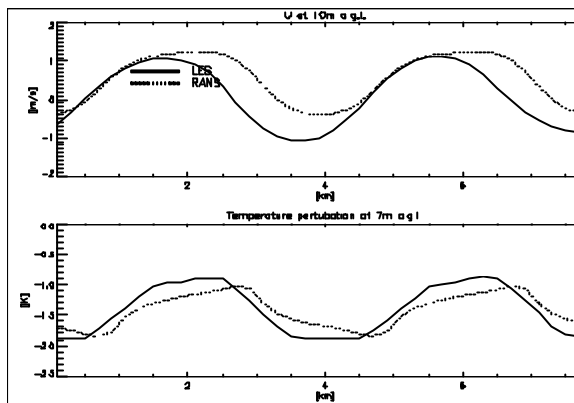


Figure 11 U and perturbation of potential temperature at the lowest model level (7m above ground) for the city case along X.

These results may indicate that PR3D overestimates the eddy viscosity in the central and upper part of the PBL. The reasons of this behavior are not clear, and may be linked also to the technique used by BouLac to estimate the length scales. Future work will be devoted to clarify this point and improve the scheme.

5. CONCLUSIONS AND OUTLOOK.

From this contribution the following conclusions can be derived:

- By controlling the value of Ra_{eff} through a modification of the effective Prandtl Number, it is possible to avoid the formation of M-CISCs, and to parameterize the CISCs (at least for homogeneous heat fluxes).
- The LES simulations show that surface heterogeneities can create ensemble mean circulations at the same scale of the turbulent motions (few kilometers). High resolution mesoscale runs should aim to simulate those features.
- The scheme based on the modification of the Prandtl number produces circulations in the right position and with wind and temperature values close to the ground, similar to those obtained by spatially averaging the LES results. However, it underestimates the vertical extent of the breezes and the magnitude of the return current.

Acknowledgements.

Thanks to Branko Kosovic (NCAR) for providing the LES results of Fig. 4.

The work of AM has been done in the framework of the project No. CGL2011-26173 funded by the Ministry of Economy and Competitiveness of the Government of Spain.

References

Bougeault, P., and P. Lacarrere, 1989: Parameterization of orography-induced turbulence in a mesobeta-scale model. *Mon. Wea. Rev.*, **117**, 1872–1890.

Ching, J., R. Rotunno, M. LeMone, A. Martilli, B. Kosovic, P. A. Jimenez, J. Dudhia, 2014: Convectively Induced Secondary Circulations in Fine-Grid Mesoscale Numerical Weather Prediction Models, under revisions for Monthly Weather Review.

Mellor, G. L., and T. Yamada, 1974: A hierarchy of turbulence closure models for planetary boundary layers. *J. Atmos. Sci.*, **31**, 1791-1806.

Pielke, R. 1984: Mesoscale Meteorological Modelling, Academic press, 600 pages.

Pope, S. 2000: Turbulent Flows, Cambridge university press, 770 pages.

Rayleigh, L., 1916: On convection currents in a horizontal layer of fluid, when the higher temperature is under side, *Phil. Mag.*, **32**, 529-546.

Shin, H. H., and S.Y Hong, 2011: Intercomparison of Planetary Boundary-Layer Parametrizations in the WRF Model for a Single Day from CASES-99, *Boundary-Layer Meteorol* **139**, 261–281

Wyngaard, J. C., 2004: Towards numerical modeling in the "Terra Incognita", *J Atmos. Sci.*, **61**, 1816-1826.

